C. R. Chimie 18 (2015) 1242–1249

Contents lists available at ScienceDirect

Comptes Rendus Chimie

www.sciencedirect.com

International Symposium on Air & Water Pollution Abatement Catalysis (AWPAC) – Catalysis for renewable energy

Dry reforming of methane over $Ni/Ce_{0.62}Zr_{0.38}O_2$ catalysts: Effect of Ni loading on the catalytic activity and on H_2/CO production

Monika Radlik [a,*], Małgorzata Adamowska-Teyssier [b,c], Andrzej Krztoń [d], Krzysztof Kozieł [a], Waldemar Krajewski [e], Wincenty Turek [a], Patrick Da Costa [b,c]

[a] Silesian University of Technology, Institute of Physical Chemistry and Technology of Polymers, M. Strzody 9, 44-100 Gliwice, Poland
[b] Sorbonne Universités, UPMC Université Paris 06, UMR 7190, Institut Jean-Le-Rond-d'Alembert, 75005 Paris, France
[c] CNRS, UMR 7190, Institut Jean-Le-Rond-d'Alembert, 75005 Paris, France
[d] Polish Academy of Sciences, Centre of Polymer and Carbon Materials, M. Curie-Sklodowskiej 34, 41-819 Zabrze, Poland
[e] Polish Academy of Sciences, Institute of Chemical Engineering, Baltycka 5, 44-100 Gliwice, Poland

ARTICLE INFO

Article history:
Received 30 November 2014
Accepted after revision 5 March 2015
Available online 30 October 2015

Keywords:
Methane
Hydrogen
Dry reforming
Ceria–zirconia
Nickel loading

ABSTRACT

The activity of ceria–zirconia-supported nickel catalysts (Ni/CZ) with various loadings of nickel (2, 4 and 10 wt. %) was studied in the case of low-temperature dry reforming of methane (DRM). XRD, S_{BET}, SEM, TPD-CO_2 and thermogravimetry were used to determine the physicochemical properties of the catalysts and of the carbon deposits formed on the surface. It was found that the agglomerates of the Ni-active phase are formed on the surface of the support for high loadings of nickel. The best conversions of CO_2 and CH_4 and an optimum ratio $H_2/CO = 1$ were obtained for the catalysts with the highest Ni content. It was also found that loading has an influence on the amount of carbon deposits formed in the DRM process.

1. Introduction

Catalytic dry reforming of methane (DRM) has received considerable attention in recent years [1–3]. In this process, two greenhouse gases are consumed, giving a synthesis gas. The advantage of this process is the molar H_2-to-CO ratio in the products, approximately equal to 1, which is suitable for many industrial processes such as production of higher hydrocarbons and oxygenated derivatives (e.g., methanol) [1–3].

The dry reforming of methane proceeds in the presence of two types of catalysts. The first group is based on noble metals such as Pt, Rh and Ru [4–6]. The second group of catalysts containing nickel is used more often in comparison with noble metals due to their low price, wide availability and satisfactory activity [1–3,7,8]. However, catalysts based on nickel show certain disadvantages – low stability and lesser H_2/CO molar ratio or decrease in activity caused by the formation of carbon deposits as a result of methane decomposition over metallic Ni-active sites [1–3,7,8]. Nickel catalysts deposited on oxide supports are used to limit the formation of carbon deposits and increase activity. MgO [9,10] and Al_2O_3 [11,12] are the most common supports. The literature data suggest that in Ni/MgO catalysts, a solid solution $Ni_x/Mg_{1-x}O$ is formed due to strong interactions between NiO and MgO. Consequently, some amount of NiO is not reduced to Ni. The small size of Ni crystallites inhibits the formation of

* Corresponding author.
E-mail address: monika.radlik@gmail.com (M. Radlik).

http://dx.doi.org/10.1016/j.crci.2015.03.008
1631-0748/

carbon deposits, while the slight number of Ni centres is responsible for the low activity in the DRM process. Therefore, high nickel loading is necessary to obtain a catalyst with sufficient activity [13–15]. The systems based on Al_2O_3 as the support show a tendency to bind Ni as a spinel ($NiAl_2O_4$), which results in the deactivation of the catalyst [16,17]. Last year, nickel deposited on hydrotalcite has been studied in detail, mainly due to great physico-chemical properties (high specific surface area, basic properties) and high activity in the DRM reaction [18,19]. Moreover, the literature data indicate that the lifetime of Ni-based catalysts can be improved by the addition of an oxide support, e.g., CeO_2 [20,21], CeO_2–ZrO_2 [22], CeO_2–SiO_2 [3], La_2O_3–ZrO_2 [8,23], CaO–ZrO_2 [24], which contain mobile lattice oxygen active in removing carbon deposits and in regenerating active sites. Literature data suggest also that catalysts based on cerium oxides show high activity and stability in the DRM process [20–22]. These systems exhibit high mobility of lattice oxygen, strong interactions with the metal and ability to change the dispersion of the active phase [3,6]. A high mobility of lattice oxygen is associated with easy changes of the oxidation state from Ce^{4+} to Ce^{3+} depending on the conditions of reduction or oxidation. Introduction of other oxides like ZrO_2 to CeO_2 increases the number of oxygen vacancies and enhances the basic properties required in the DRM process [1,6].

Temperature is another important factor that affects the activity and stability of Ni-based catalysts. Since DRM is an endothermic process, higher temperature improves the conversion of both CH_4 and CO_2, but can also cause deactivation of the catalyst due to the formation of carbon deposits [1,8]. Moreover, maintaining a rational cost of DRM is possible only if the process can be carried out at temperatures below 550 °C [1,8]. Very few works concerning low-temperature DRM have been published so far [23–25].

Literature data indicate that the catalytic activity and the amount of carbon deposits depend on the morphology, the size and the dispersion of Ni particles on the surface of the support [5,6,8,26,27]. It seems that high dispersion of the active phase on the surface of the support restricts the formation of carbon deposits [9,26]. More carbon deposits are formed at the surface of big Ni crystallites. The interaction with the support is also important, because it can change the number of active sites and the activity of Ni-based catalysts in DRM [9].

The aim of this work is to study the activity of catalysts containing nickel deposited on the ceria–zirconia mixed oxide support (CZ) in the low-temperature DRM (550 °C). Barroso-Quiroga and Castro-Luna have recently studied the activity of Ni catalysts (10 wt. %) supported on oxides like CeO_2 and ZrO_2 at low-temperature DRM at 550 °C [25]. However, no literature data concerning the activity of nickel supported on ceria–zirconia mixed oxide catalysts in DRM at a temperature of 550 °C have been found. Therefore, for these purposes, catalysts containing various amounts of the nickel active phase (2, 4 and 10 wt. %) deposited on the ceria–zirconia mixed oxide support $Ce_{0.62}Zr_{0.38}O_2$ were synthesized. The physicochemical properties of the catalysts were characterized using XRD, S_{BET}, SEM and CO_2-TPD techniques. The low-temperature DRM tests were performed at 550 °C for 5 h. After the process, the catalysts were characterized using XRD and TG analysis to evaluate the amount and the character of carbon deposits. Special attention was given to the influence of variable loading with the active phase on the activity and selectivity of the catalysts in dry reforming of methane at low temperature (550 °C).

2. Experimental

2.1. Catalyst preparation

A series of $NiO/Ce_{0.62}Zr_{0.38}O_2$ (named as Ni/CZ) catalysts with different amounts of nickel were prepared by incipient wetness impregnation of the commercial ceria–zirconia support (provided by Rhodia Electronics & Catalysts) with the nickel nitrate aqueous solution. Next, the samples were dried in the air at 120 °C for 12 h and finally calcined at 550 °C for 2 h. The amount of Ni was 2, 4 and 10 wt. %. The obtained catalysts were denoted as Ni(2)/CZ, Ni(4)/CZ and Ni(10)/CZ, respectively.

2.2. Characterization of the catalyst and of the support

X-ray diffraction (XRD) experiments were performed on a Siemens D5005 (Bruker-AXS, Germany) apparatus with Cu Kα radiation, operating at 30 kV and 50 mA. The X-ray powder diffractogram was recorded in the 2θ range between 20 and 90°.

The Brunauer–Emmet–Teller (BET) surface area and the pore volume of the studied catalysts and of the support were obtained by N_2 adsorption at 77.35 K using a BELSORP MINI adsorption apparatus. Before the measurements, the samples were degassed at 110 °C until a stable vacuum of ca. 10^{-3} Pa was reached.

SEM analysis was performed using a SEM QUANTA 250 FEG (FEI, USA) microscope equipped with an EDS detector (type SDD Apollo 10, EDAX) with a resolution of 129.11 eV. The measurements of the Ni/CZ catalysts and support were carried out in high vacuum, under an acceleration voltage equal to 10 kV using an LFD (SED/BSED) detector. The chemical composition of the examined samples was established by using the EDS detector under an acceleration voltage of 30 kV.

The CO_2-TPD was performed on a BELCAT-M apparatus. Prior to the TPD experiment, the catalyst (0.05–0.06 g) was first degassed for 2 h at 500 °C and then cooled to 50 °C. Adsorption of CO_2 was performed by passing a flow of 10% v/v CO_2/He with a flow rate of 50 mL/min through the sample bed at 50 °C for 1 h. In the next step, a flow of He was subsequently fed for 15 min in order to desorb the weakly physically adsorbed CO_2. The CO_2-TPD measurements were carried out under He up to 900 °C, with a heating rate of 10 °C/min.

After the DRM tests, the catalysts were characterized by XRD and thermogravimetric analysis (TG) to examine the formation of carbon deposits. The procedure of XRD analysis was described in detail above. TG analysis was

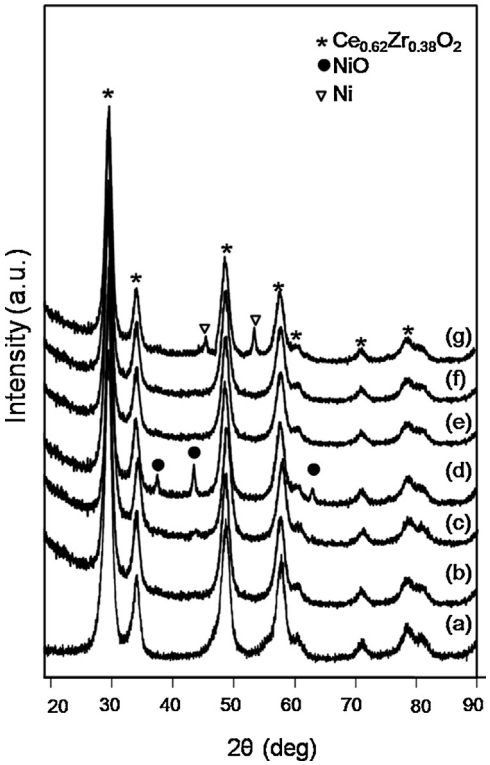

Fig. 1. X-ray diffraction patterns of the catalysts treated in different conditions. Calcined catalysts ceria–zirconia (CZ) (a), Ni(2)/CZ (b), Ni(4)/CZ (c), Ni(10)/CZ (d) and after reduction in H_2/Ar Ni(2)/CZ (e), Ni(4)/CZ (f), Ni(10)/CZ (g).

performed using a thermogravimetric analyser Derivatograph Q-1500, MOM Budapest. The used catalysts were heated from 20 to 940 °C at the rate of 10 °C/min; the weight loss was monitored simultaneously.

2.3. Catalytic dry reforming tests

The evaluation of the catalysts was carried out in a quartz fixed-bed reactor. Before the experiments, the catalyst was reduced *in situ* at 800 °C for 2 h with 3% vol. H_2 in Ar at a flow rate of 100 mL/min. The reaction mixture with the molar ratio $CO_2/CH_4/Ar = 1/1/8$ was controlled using a Brooks mass flow meter. The GHSV was 20,000 h^{-1}. The exhaust gases were analyzed with a micro gas chromatograph, Varian CPi 4900, equipped with COX column, and a thermal conductivity detector.

3. Results and discussion

3.1. XRD phases of catalysts and support

The X-ray diffraction results of the pure support and calcined catalysts are presented in Fig. 1a–d. The XRD patterns of the support exhibit planes at (111), (200), (220), (311), (222), (400) and (420) characteristic of the fluorite cubic structure of ceria–zirconia mixed oxides [28]. It can be observed that planes characteristic of the regular structure of the support are present in all Ni/CZ diffractograms. Plane characteristics of the regular structure of nickel oxide (111), (002), (022), (113) (JCDPS 01-073-1519) were observed only for Ni(10)/CZ (Fig. 1d). Thus, Ni/CZ catalysts with low loading of the active phase probably contain well-dispersed NiO crystallites, so the respective signals were not recorded during XRD measurements. Table 1 shows the size of crystallites and lattice parameters of calcined Ni/CZ catalysts and of the support. The crystallite size of NiO in Ni(10)/CZ is almost 2 times higher than for pure CZ. For Ni(2)/CZ and Ni(4)/CZ, the size of NiO crystallites was probably much lower than in Ni(10)/CZ, and presumably even lower than in the CZ support. The size of the crystallites of the support was larger than for Ni/CZ catalysts. This effect can be caused by increasing the crystallographic disorder in the structure of the support after impregnation [29]. The lattice parameters of the support were smaller than the respective values observed for Ni/CZ catalysts and decreased for higher loading with the active phase. It can be caused by substitution of Ce^{4+} ions (ionic radius 0.097 nm) with smaller Ni^{2+} ions (ionic radius 0.069 nm) [29,30].

Since the active sites in the DRM process are metallic centres, the Ni/CZ catalysts and the support need to be reduced. Before XRD measurements, the samples were reduced in 3% H_2/Ar at 800 °C for 2 h. Fig. 1e–f shows XRD diffractograms of Ni/CZ catalysts after reduction. Table 1 contains the parameters for Ni crystallites for Ni/CZ catalysts after reduction, calculated from the Scherer equation. The diffraction patterns contained no planes characteristic of the regular nickel oxide structure. In the case of Ni(10)/CZ catalyst, reflexions characteristic of metallic Ni (JCDPS 87-0712) were visible. It proves that NiO crystallites were completely reduced to Ni^0. These planes were not observed for other Ni/CZ catalysts, which can be caused by the high dispersion of small Ni crystallites on the surface of the support (Table 1). Large Ni particles were formed in the case of the catalyst Ni(10)/CZ (Table 1). Hence, in the diffraction pattern of Ni(10)/CZ (Fig. 2g),

Table 1
Structural properties of calcined and reduced samples.

Catalyst	Calcined samples			Reduced samples		
	Crystallite size CZ (nm)	Crystallite size NiO (Å)	Lattice of CZ (Å)	Crystallite size CZ (nm)	Crystallite size Ni (Å)	Lattice of CZ (Å)
CZ	7.91	–	5.32	7.92	–	5.32
Ni(2)/CZ	7.67	–	5.31	7.73	–	5.33
Ni(4)/CZ	7.66	–	5.31	7.72	–	5.32
Ni(10)/CZ	7.71	17.27	5.31	7.90	18.41	5.31

CZ: ceria–zirconia; Ni: nickel.

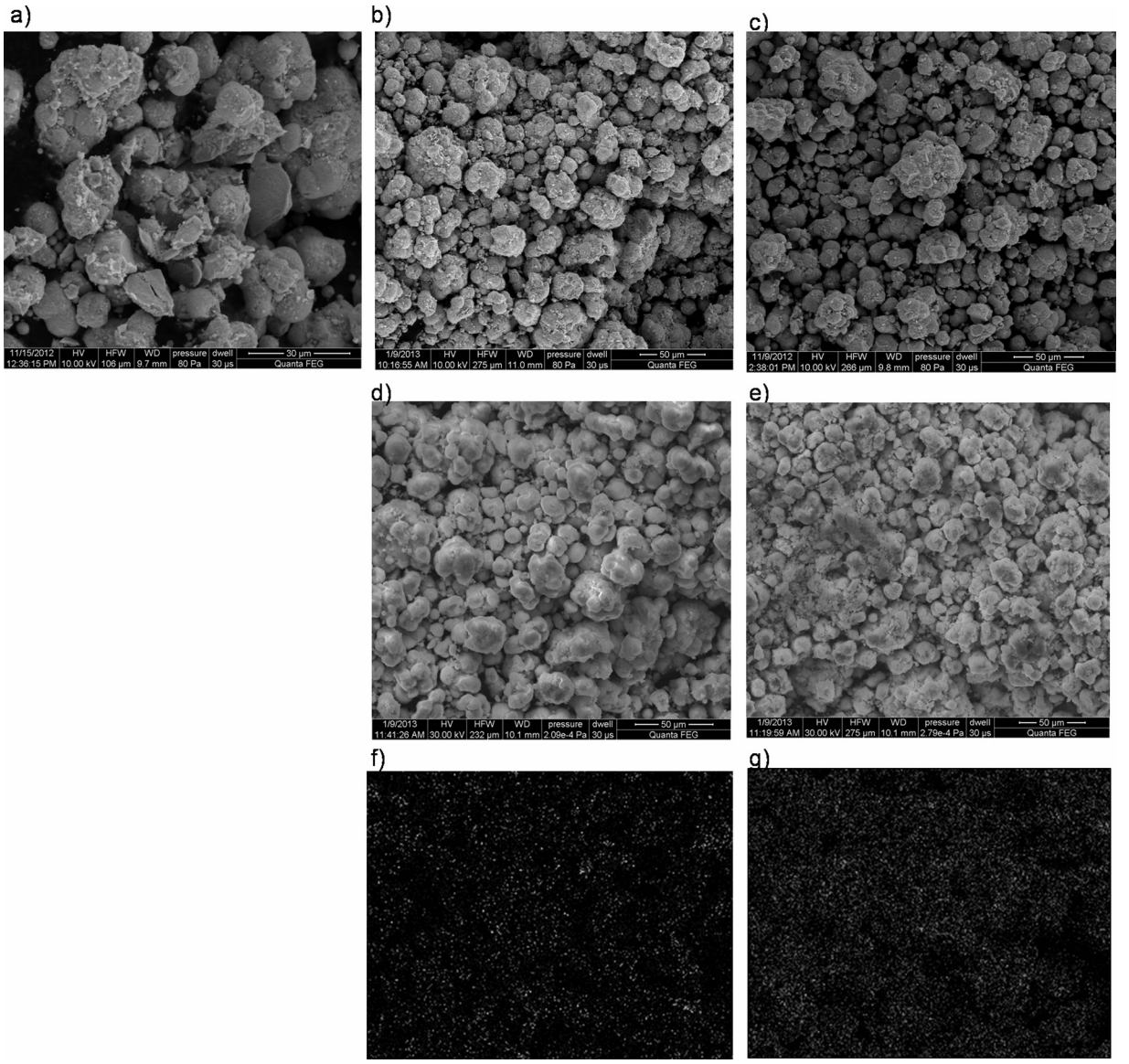

Fig. 2. SEM images of ceria–zirconia (CZ) (a) Ni(4)/CZ (b, d) and Ni(10)/CZ (c, e) with elemental mapping of Ni [Ni(4)/CZ (f) and Ni(10)/CZ (g)].

reflexions originating from Ni^0 particles were visible. The sizes of the crystallites of Ni and of the support were greater than in the case of calcined samples, due to the sintering observed during the reduction process.

3.2. Specific surface area and scanning electron microscopy

Table 2 shows the values of specific surface area (SSA) of the support and calcined Ni/CZ catalysts. The SSA of the support, equal to 125 m^2/g, was the highest among the samples studied. The calcined catalysts Ni/CZ exhibit a slight decrease in the specific surface area for higher loading with the active phase. The decrease in the specific surface area can be explained by blocking pores of the support by the active phase (NiO). The SSA of Ni/CZ catalysts was similar, and the lowest value was observed for Ni(10)/CZ. It may be explained by the large-size NiO crystallites on the surface of the support and lower dispersion, which was confirmed by XRD results (Table 1). The values of pore size for the support and NiO/CZ catalysts were presented in Table 2. Additionally, it can be observed that the CZ pore volume was higher compared to that in Ni/CZ systems. The pore volumes of Ni(2)/CZ and Ni(4)/CZ samples are identical and lower in comparison to those in Ni(10)/CZ. In all catalysts, smaller grains of nickel oxide block the pores of the support.

Fig. 2 shows SEM images of the CZ (Fig. 2a), Ni(4)/CZ (Fig. 2b and d) and Ni(10)/CZ (Fig. 2c and e) with elemental map of Ni (Fig. 2f and g). The Ni(4)/CZ and Ni(10)/CZ catalysts has been selected as representative, because no differences between Ni(2)/CZ and Ni(4)/CZ were observed by SEM. The SEM images of the studied catalysts show that

Table 2
BET specific surface area, total pore volume, average pore diameter and amount of desorbed CO_2 during CO_2-TPD.

Catalyst	BET surface area (m^2/g)	Pore volume (cm^3/g)	Average pore diameter (nm)	Amount of desorbed CO_2 ($mmol/g_{cat}$)
CZ	125	0.28	8.8	0.18
Ni(2)/CZ	92	0.26	11.2	0.20
Ni(4)/CZ	87	0.26	12.0	0.21
Ni(10)/CZ	83	0.22	10.5	0.23

BET: Brunauer–Emmet–Teller; TPD: temperature-programmed desorption; CZ: ceria–zirconia; Ni: nickel.

they consist of big particles, which can be ascribed to the particles of the support, and of smaller particles of NiO. The SEM images with an elemental map of Ni (Fig. 2f and g) indicate a better dispersion of the Ni phase for the sample with lower Ni loading. When the amount of Ni was 10 wt. %, the formation of NiO agglomerates can be observed on the surface of the support, which is confirmed by XRD results (Fig. 1).

3.3. Basicity of Ni/CZ catalysts and support

The basic properties of the catalyst surface play an important role in the DRM process, since they are required in the adsorption and activation of CO_2 [3]. They can be studied by temperature-programmed desorption of CO_2 (TPD-CO_2). Before the CO_2-TPD measurement, the samples were reduced in a stream of 5% H_2/Ar at 800 °C and the results of TPD-CO_2 for Ni/CZ catalysts and the support are presented in Fig. 3. The pure support showed a strong desorption contour, which was deconvoluted into the three desorption components. The first contour component observed in the temperature range 50–150 °C can be ascribed to the presence of basic centres of low strength (e.g., OH) [24,29–33]. The second component, with a maximum at around 200 °C, can be ascribed to the desorption of CO_2 from the basic sites of medium strength (metal–oxygen pairs) [34,35]. The next desorption profile with a maximum at 350 °C can be associated with the presence of relatively strong basic sites (e.g., O^{2-}) [32,33]. In the case of the catalysts, desorption contours were noticed in the temperature range from 450 to 700 °C. TPD large profile results of CO_2 desorption from Ni/CZ are resolved also into three separated components. It should be mentioned that for Ni/CZ catalysts, similar temperatures of CO_2 desorption for all the samples indicate the presence of basic sites of similar strength. The literature data report that in the temperature range from 300 to 600 °C, CO_2 is desorbed from metallic Ni sites. Therefore, the peaks with the maximum at approximately 500 °C, observed for Ni/CZ catalysts, can be ascribed to the desorption of CO_2 from metallic nickel centers [36–38]. Subsequent desorption contour components are associated with the presence of medium [34,35] and strong basic sites [20–22]. Thus, incorporation of nickel leads to the formation of strong basic sites and the elimination of weak basic ones. The numbers of basic sites (Table 2) were found higher for Ni/CZ catalysts than the respective number for the pure support. These phenomena can be explained by

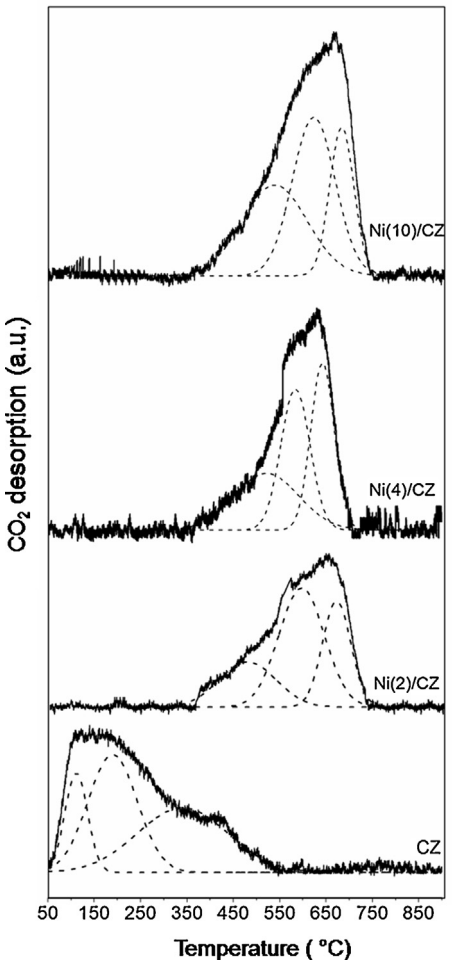

Fig. 3. CO_2-temperature-programmed desorption profile of ceria–zirconia (CZ) (a) and reduced catalysts Ni(2)/CZ (b), Ni(4)/CZ (c), Ni(10)/CZ (d).

the strong interaction between Ni and ceria, which can enhance the basicity of Ni/CZ catalysts. According to the literature, addition of Ni into the ceria–zirconia improved the redox properties of the material, favouring oxygen transfer, which would be required for CO_2 activation [32,39–41].

3.4. Catalytic DRM tests

Figs. 4 and 5 show the conversion of CH_4 and CO_2, respectively as a function of time during the DRM at a temperature of 550 °C for the catalysts Ni/CZ. The highest conversion rate of methane and carbon dioxide at 550 °C was observed for the Ni(10)/CZ catalyst. Other Ni/CZ catalysts showed lower conversion and H_2/CO molar ratio. High activity of the Ni(10)/CZ catalyst, in comparison with other samples, may be caused by the high loading of the active phase and a greater number of active sites. Other important factors were the differences in size and dispersion of the active phase crystallites. It has been proved that the size and dispersion of Ni crystallites affect the activity Ni-based catalysts in DRM [1,26,43]. For the

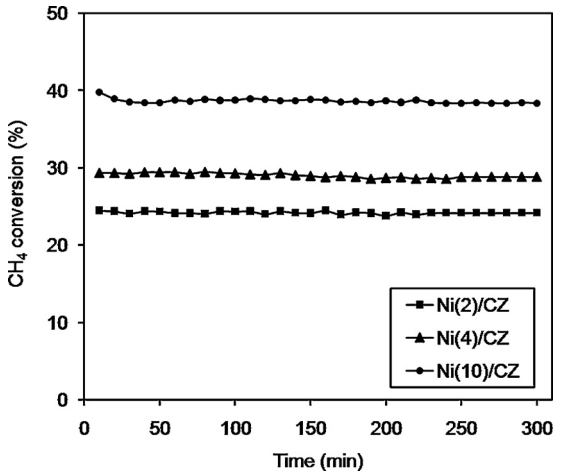

Fig. 4. CH_4 conversions over different catalysts: Ni(2)ceria–zirconia (CZ), Ni(4)/CZ and Ni(10)/CZ. Reaction conditions: $CH_4/CO_2/Ar = 1/1/8$; GHSV = 20,000 h^{-1}; catalysts were reduced in H_2/Ar 3 v/v % Ar at 800 °C for 2 h.

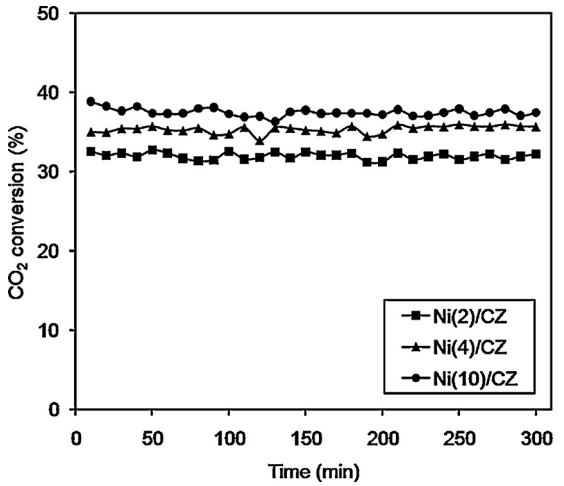

Fig. 5. CO_2 conversions over different catalysts: Ni(2)ceria–zirconia (CZ), Ni(4)/CZ and Ni(10)/CZ. Reaction conditions: $CH_4/CO_2/Ar = 1/1/8$; GHSV = 20,000 h^{-1}; catalysts were reduced in H_2/Ar 3 v/v % Ar at 800 °C for 2 h.

calcined Ni/CZ catalysts, the XRD and SEM results suggested that at low loading, the active phase existed in the form of small and highly dispersed crystallites. High dispersion of the active phase on the surface of the support affected not only the physicochemical properties of the catalysts, but also the number of metallic Ni^0 active sites. When NiO crystallites were well-dispersed, this could have a profound effect on the strong interactions between the active phase and the support. Such interactions may hinder the reduction of NiO crystallites to the active form of metallic Ni^0 [1,26,43] and consequently lower the activity of the catalysts in the DRM process, for the calcined Ni(10)/CZ active phase favoured the formation of large Ni crystallites of low dispersion (which was proved by XRD and SEM analyses). It is associated with a difficult access of the NiO phase to the support and weakness interactions of the active phase with the support. Therefore, for Ni(10)/CZ, we can expect to increase the conversion of CH_4 in comparison with the other studied Ni/CZ catalysts. A similar trend was also observed for the conversion of CO_2 (Fig. 5). It can be associated with the increasing basicity of the catalyst (Table 2). Hence, Ni(10)/CZ showed higher conversion of CH_4 and CO_2 in comparison to the catalyst with lower Ni content.

In this study, ceria–zirconia was used as the support. The pure support was not active in the DRM process and these results are not presented in this work. However, its role in the DRM process is important, because of unique physicochemical properties. The literature data proved that CeO_2 can easily change the oxidation state [3,6]. Addition of ZrO_2 increases the hydrothermal stability and the basic properties required in the DRM process [1,4,6]. Moreover, introduction of some zirconium atoms in the ceria lattice by substitution of some Ce^{4+} ions with Zr^{4+} ions creates oxygen vacancies and increases the mobility of lattice oxygen from the bulk of the catalyst to its surface. The presence of oxygen vacancies and the surface oxygen is important for the activity of the catalysts in the DRM reaction. Numerous papers showed that the activation of methane occurs over metallic active centres and the activation of CO_2 takes place over oxygen vacancies or surface oxygen of the support [22,27,42]. It has been proved that CeO_2 enhances nickel–support interactions and increases the dispersion of Ni [23,43,44]. Therefore, the role of the CZ support in the DRM is significant.

Fig. 6 shows the H_2-to-CO molar ratio in the DRM process for the support and Ni/CZ catalysts. It is well known that the molar ratio H_2/CO depends on concurrent reactions. The literature data indicate that these processes are reverse water-gas shift (RWGS) [3,17,24,43,45], decomposition of methane [3,9,17,24,45] and Boudouard reactions [3,24,45]. According to our results the best value of the H_2/CO molar ratio (equal to 1) was observed for the Ni(10)/CZ catalyst. For other Ni/CZ catalysts, the ratio H_2/CO was below 1 and also

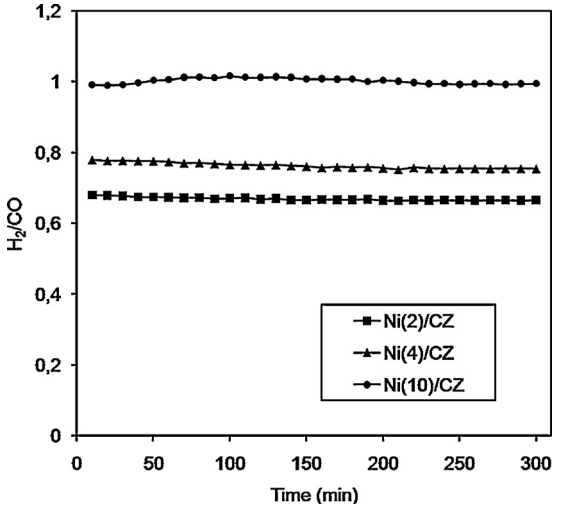

Fig. 6. H_2/CO molar ratio over Ni(2)ceria–zirconia (CZ), Ni(4)/CZ and Ni(10)/CZ. Reaction conditions: $CH_4/CO_2/Ar = 1/1/8$; GHSV = 20,000 h^{-1}; catalysts were reduced in H_2/Ar 3 v/v % Ar at 800 °C for 2 h.

more carbon dioxide than methane was used in the reaction (which lowers the value of H_2/CO molar ratio). This phenomenon was caused by a competitive reaction of reverse water-gas shift (RWGS) in which a fraction of produced hydrogen reacts with CO_2, yielding CO and water ($CO_2 + H_2 = CO + H_2O$) and giving an H_2/CO molar ratio below 1 [1–3,20,38].

3.5. Characterization of catalysts after DRM tests

After DRM experiments, the catalysts were characterized using XRD and thermogravimetric analysis to identify and estimate the amount of formed carbon material. Fig. 7 shows the XRD results for catalysts obtained after the DRM experiment. The diffraction patterns indicate that all the catalysts showed reflexes typical of the regular structure of cerium oxide. Reflexes coming from the structure of Ni^0 (JCDPS 87-0712) were found in the spectra of Ni(10)/CZ. In the case of Ni(10)/CZ, reflexes originating from carbon deposits at 2θ 26.5 (JCDPS 26-1080) were visible. Other Ni/CZ catalysts did not shown any reflexes in this range. It can be caused by the lack of carbon deposits on the surface of the catalysts or by their formation in very low amounts.

Thermogravimetric analyses were preformed to evaluate the amount of carbon formed on the surface of the catalysts. The mass decrease observed on the TG curves is caused by the oxidation of carbon deposits to CO_2. A higher mass decrease indicates a greater amount of carbon on the surface. Fig. 8 shows TG plots in the form of percentage of mass decrease as a function of temperature. The highest mass decrease, equal to 40%, was observed in the case of the Ni(10)/CZ catalyst. For other catalysts – Ni(2)/CZ and Ni(4)/CZ – the mass decreased by 5 and 10 wt. %, respectively. It proved that the highest amount of carbon deposits was produced on the surface of Ni(10)/CZ, which is also confirmed by the XRD results (Fig. 7).

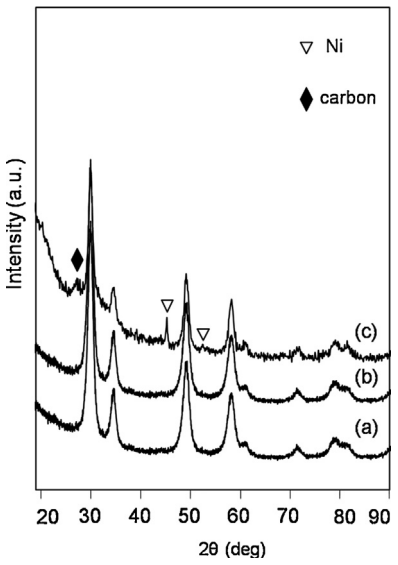

Fig. 7. X-ray diffraction patterns of the spent catalysts: Ni(2)/ceria–zirconia (CZ) (a), Ni(4)/CZ (b) and Ni(10)/CZ (c).

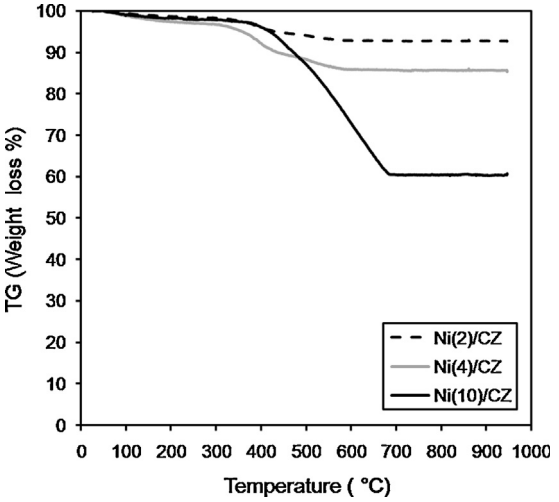

Fig. 8. Thermogravimetric analysis plots of the spent catalysts.

Carbon deposits in DRM can be formed as a result of the disproportionation of CO in the Boudouard reaction ($2\ CO = C + CO_2$) [3,24,45] or methane cracking ($CH_4 = C + 2H_2$) over metallic sites [3,9,17,45]. Therefore, the amount of carbon deposits should increase with higher loading with the active phase. This relationship was observed for Ni/CZ catalysts, but the increase was not proportional to the loading of Ni and the amount of carbon deposits was much higher for Ni(10)/CZ than for other catalysts. It can be caused by the large crystallites of the active phase on the surface of the support. Literature data showed that large crystallites of Ni enhance the formation of carbon deposits [6,21,26]. It was proved that large Ni particles have hindered contact with the lattice oxygen and limited removal of carbon deposits [6,21,26]. Thus, a higher amount of carbon deposits was formed on the surface of Ni(10)/CZ in comparison with other Ni/CZ catalysts.

It is worth noting that the carbon deposits can be oxidized to CO by gaseous CO_2 in the reverse Boudouard reaction ($C + CO_2 \rightarrow 2\ CO$) [23,24] or to CO_2 by the surface oxygen of the support ($C + O_2 \rightarrow CO_2$) [20–24]. It has been proved that these reactions have an influence on the molar ratio H_2/CO [20–24]. Hence, the lower value of the molar ratio $H_2/CO < 1$, observed for Ni(2)/CZ and Ni(4)/CZ catalysts, can be caused by RWGS reaction and oxidation of carbon deposits by CO_2. Oxidation of carbon deposits by CO_2 in the reverse Boudouard reaction can also occur over the catalyst Ni(10)/CZ. This reaction can change the value of the molar ratio H_2/CO obtained in the DRM process over Ni(10)/CZ.

4. Conclusion

A series of Ni/CZ catalysts containing 2, 4 and 10 wt. % of nickel was obtained using incipient wetness impregnation. The catalysts and the support were characterized by XRD, BET, and CO_2-TPD. The activity of the catalysts in low-temperature DRM at a temperature of 550 °C was investigated. XRD and SEM results indicated that high

loading with nickel leads to the formation of large crystallites of the active phase with lower dispersion. Catalytic DRM tests showed that the highest conversion of CH_4 and CO_2 and an optimum ratio $H_2/CO = 1$ were obtained in the case of the Ni(10)/CZ catalyst. It has been demonstrated that the physicochemical properties and activity of Ni/CZ catalysts depend on the size of the Ni crystallites on the surface of the support. An increasing basicity of the catalysts with higher Ni contents was observed. The competitive reaction of RWGS and reverse Boudouard reaction were observed for Ni/CZ catalysts. It was demonstrated that the presence of big Ni crystallites promoted the decomposition of CH_4 and the formation of carbon deposits.

References

[1] D. Harshini, D. Hyung, L.Y. Kim, S.W. Nam, J.H. Han, H.C. Ham, C.W. Yoon, Catal. Lett. 144 (2014) 656.
[2] A.R. Derk, G.M. Moore, S. Sharma, E.W. McFarland, H. Metiu, Top. Catal. 57 (2014) 118.
[3] Y.H. Taufiq-Yap, Sudarno, U. Rashid, Z. Zainal, Appl. Catal., A: Gen. 468 (2013) 359.
[4] D. Pakhare, J. Spivey, Chem. Soc. Rev. 43 (2014) 7813.
[5] Z. Ferencz, K. Baán, A. Oszkó, Z. Kóny, T. Kecskés, A. Erdöhelyi, Catal. Today 228 (2014) 123.
[6] A.S. Bobin, V.A. Sadykov, V.A. Rogov, N.V. Mezentseva, G.M. Alikina, E.M. Sadovskaya, T.S. Glazneva, N.N. Sazonova, M. Yu Smirnova, S.A. Veniaminov, C. Mirodatos, V. Galvita, G.B. Marin, Top. Catal. 56 (2013) 958.
[7] B. Bachiller-Baeza, C. Mateos-Pedrero, M.A. Soria, A. Guerrero-Ruiz, U. Rodemerck, I. Rodríguez-Ramos, Appl. Catal., B: Environ. 129 (2013) 450.
[8] S. Sokolov, E.V. Kondratenko, M.M. Pohl, U. Rodemerck, Int. J. Hydrogen Energy 38 (2013) 16121.
[9] R. Zanganeh, M. Rezaei, A. Zamaniyan, Adv. Powder Technol. 25 (2014) 1111.
[10] L. Li, L. Zhang, X. Shi, Y. Zhang, J. Li, J. Porous Mater. 21 (2014) 217.
[11] A.E. Castro-Luna, M.E. IriaRTE, Appl. Catal., A: Gen. 343 (2008) 10.
[12] W. Chen, G. Zhao, Q. Xue, L. Chen, Y. Lu, Appl. Catal., B: Environ. 1236–137 (2013) 260.
[13] F. Arena, B.A. Horrell, D.L. Cocke, A. Parmaliana, N. Giordano, J. Catal. 132 (1991) 58–67.
[14] E. Ruckenstein, Y.H. Hu, Appl. Catal., A: Gen. 133 (1995) 149.
[15] K. Sutthiumporn, S. Kawi, Int. J. Hydrogen Energy 36 (2011) 14435.
[16] B. Pawelec, P. Castaño, J.M. Arandes, J. Bilbao, S. Thomas, M.A. Peña, J.L.G. Fierro, Appl. Catal., A: Gen. 317 (2007) 20.
[17] S. Damyanova, B. Pawelec, K. Arishtirova, J.L.G. Fierro, Int. J. Hydrogen Energy 37 (2012) 15966–15975.
[18] C.E. Daza, J. Gallego, J.A. Moreno, F. Mondragón, S. Moreno, R. Molina, Catal. Today 133 (2008) 357.
[19] R. Dębek, A. Gramatyka, M. Motak, P. Da Costa, Przem. Chem. 93 (2014) 2026.
[20] V.M. Gonzalez-Delacruz, F. Ternero, R. Perẽniguez, A. Caballero, J.P. Holgado, Appl. Catal., A: Gen. 384 (2010) 1.
[21] T. Odedairo, J. Chen, Z. Zhu, Catal. Commun. 31 (2013) 25.
[22] A. Kambolis, H. Matralis, A. Trovarelli, C. Papadopoulou, Appl. Catal., A: Gen. 377 (2010) 16.
[23] S. Sokolov, E.V. Kondratenko, M.M. Pohl, A. Barkschat, U. Rodemerck, Appl. Catal., B: Environ. 113–114 (2012) 19.
[24] N. Sun, X. Wen, F. Wang, W. Peng, N. Zhao, F. Xiao, W. Wei, Y. Sun, J. Kang, Appl. Surf. Sci. 257 (2011) 9169.
[25] M.M. Barroso-Quiroga, A.E. Castro-Luna, Int. J. Hydrogen Energy 35 (2010) 6052.
[26] R. Zanganeh, M. Rezaei, A. Zamaniyan, Int. J. Hydrogen Energy 38 (2013) 3012.
[27] B.M. Nagaraja, D.A. Bulushev, S. Beloshapkin, S. Chansai, J.R.H. Ross, Top. Catal. 56 (2013) 1686.
[28] M. Radlik, M. Adamowska, A. Łamacz, A. Krztoń, P. Da Costa, W. Turek, Reac. Kinet. Mech. Catal. 109 (2013) 43.
[29] B.M. Reddy, P. Bharali, G. Thrimurthulu, P. Saikia, L. Katta, S.E. Park, Catal. Lett. 123 (2008) 327.
[30] F. Ocampo, B. Louis, L. Kiwi-Minsker, A.C. Roger, Appl. Catal., A: Gen. 392 (2011) 36.
[31] J.M. García-Vargas, J.L. Valverde, A. de Lucas-Consuegra, B. Gómez-Monedero, P. Sánchez, F. Dorado, Appl. Catal., A: Gen. 431–432 (2012) 49.
[32] P.V.R. Rao, V.P. Kumar, G.S. Rao, K.V.R. Chary, Catal. Sci. Technol. 2 (2012) 1665.
[33] J. Gao, J. Guo, D. Liang, Z. Hou, J. Feia, X. Zheng, Int. J. Hydrogen Energy 33 (2008) 5493.
[34] A.H. de Morais Batista, F.S.O. Ramos, T.P. Braga, C.L. Lima, F.O.F. de Sousa, E.B.D. Barros, J.M. Filho, A.S. de Oliveira, J.R. de Sousa, A. Valentini, A.C. Oliveira, Appl. Catal., A: Gen. 3682 (2010) 148.
[35] L. Zhao, X. Li, Z. Qu, Q. Zhao, S. Liu, X. Hu, Separ. Purif. Technol. 80 (2011) 345.
[36] O. Bergada, P. Salagre, Y. Cesteros, F. Medina, J. Sueiras, Catal. Lett. 122 (2008) 259.
[37] S.C. Dantas, J.C. Escritori, R.R. Soares, C.E. Horli, Chem. Eng. J. 156 (2010) 380.
[38] J.M. García-Vargas, J.L. Valverde, F. Dorado, P. Sánchez, J. Mol. Catal. A: Chem. 395 (2014) 108.
[39] S.C. Dantas, J.C. Escritori, R.R. Soares, C.E. Hori, Chem. Eng. J. 156 (2010) 380.
[40] Q. Pan, J. Peng, T. Sun, D. Gao, S. Wang, S. Wang, Fuel Process. Technol. 123 (2014) 166.
[41] H.-S. Roh, H.S. Potdar, K.-W. Jun, J.-W. Kim, Y.-S. Oh, Appl. Catal., A: Gen. 276 (2004) 231.
[42] Y.J.O. Asencios, E.M. Assaf, Fuel Process. Technol. 106 (2013) 247.
[43] B. Koubaissy, A. Pietraszek, A.C. Roger, A. Kiennemann, Catal. Today. 157 (2010) 436.
[44] J. Chen, R. Wang, J. Zhang, F. He, S. Han, J. Mol. Catal. A: Chem. 235 (2005) 302.
[45] M. García-Diéguez, I.S. Pieta, M.C. Herrera, M.A. Larrubia, L.J. Alemany, J. Catal. 270 (2010) 136.